Homeopathy (2010) 99, 231–242

doi:10.1016/j.homp.2010.05.006, available online at http://www.sciencedirect.com

ORIGINAL PAPER

Extreme homeopathic dilutions retain starting materials: A nanoparticulate perspective

Prashant Satish Chikramane[1], Akkihebbal K Suresh[1,2], Jayesh Ramesh Bellare[1,2,*] and Shantaram Govind Kane[1,*]

[1]*Department of Chemical Engineering, Indian Institute of Technology (IIT), Bombay, Adi Shankaracharya Marg, Powai, Mumbai 400 076, Maharashtra, India*
[2]*Department of Biosciences and Bioengineering, Indian Institute of Technology (IIT), Bombay, Adi Shankaracharya Marg, Powai, Mumbai 400 076, Maharashtra, India*

Homeopathy is controversial because medicines in high potencies such as 30c and 200c involve huge dilution factors (10^{60} and 10^{400} respectively) which are many orders of magnitude greater than Avogadro's number, so that theoretically there should be no measurable remnants of the starting materials. No hypothesis which predicts the retention of properties of starting materials has been proposed nor has any physical entity been shown to exist in these high potency medicines. Using market samples of metal-derived medicines from reputable manufacturers, we have demonstrated for the first time by Transmission Electron Microscopy (TEM), electron diffraction and chemical analysis by Inductively Coupled Plasma-Atomic Emission Spectroscopy (ICP-AES), the presence of physical entities in these extreme dilutions, in the form of nanoparticles of the starting metals and their aggregates. *Homeopathy* (2010) **99**, 231–242.

Keywords: Homeopathy; Nanoparticles; Nanocrystalline materials; Transmission Electron Microscopy

Introduction

Homeopathy, a mode of therapy, was established in the late 18th century by German physician, Samuel Hahnemann. Hahnemann, during his experiments, prepared medicines from a wide variety of natural products. He discerned that the infinite dilutions of these substances carried out in steps and accompanied by vigorous shaking 'succussion' (together known as potentization) at each dilution step, elicited some kind of a potent activity to these solutions.[1,2] In spite of the various controversies and frequent challenges by the scientific community regarding its efficacy, this mode of treatment has stood the test of time, and is still being used in many countries for treatment of various chronic conditions, with medicines being prepared from a variety of herbal, animal, metal and other mineral sources.

*Correspondence: Jayesh Ramesh Bellare and Shantaram Govind Kane, Department of Chemical Engineering, Indian Institute of Technology (IIT), Bombay, Adi Shankaracharya Marg, Powai, Mumbai 400 076, Maharashtra, India.
E-mail: jb@iitb.ac.in, sgkane@gmail.com
Received 6 November 2009; revised 22 April 2010; accepted 22 May 2010

However, a major lacuna has been the lack of evidence of physical existence of the starting material. The main difficulty in arriving at a rational explanation stems from the fact that homeopathic medicines are used in extreme dilutions, including dilution factors exceeding Avogadro's number by several orders of magnitude, in which one would not expect any measurable remnant of the starting material to be present. In clinical practice, homeopathic potencies of 30c and 200c having dilution factors of 10^{60} and 10^{400} respectively, far beyond Avogadro's number of 6.023×10^{23} molecules in one mole, are routinely used.

Many hypotheses have been postulated to justify and elucidate their mechanisms of action. While some hypotheses such as the theory of water memory,[3–5] formation of clathrates,[6] and epitaxy[7] are conjectural in nature, others such as those based on the quantum physical aspects of the solutions[8,9] have not been sufficiently tested, either due to complexity in validating the hypothesis or due to non-reproducible results. The 'silica hypothesis'[10] is the only model that proposes the presence of physical entities such as siloxanes or silicates resulting from leaching from the glass containers. Following a dearth of credible and testable hypotheses to identify any physical entity responsible for medicinal activity, most modern scientists continue to believe that homeopathy at best provides a placebo effect.

Despite the extreme dilutions in 30c and 200c potencies, our approach has been to test for the presence of the starting materials in the form of nanoparticles.. Medicines selected were metal-based, and were so chosen that the metals would not arise either as impurities or as contaminants. The six metals and their respective homeopathic medicines were gold (*Aurum metallicum* or *Aurum met*), copper (*Cuprum metallicum* or *Cuprum met*), tin (*Stannum metallicum* or *Stannum met*), zinc (*Zincum metallicum* or *Zincum met*), silver (*Argentum metallicum* or *Argentum met*) and platinum (*Platinum metallicum* or *Platinum met*). Three potencies: 6c, 30c, and 200c were selected. The dilution factor for 6c is 10^{12} which is less than Avogadro's number, whereas the dilution factors for 30c and 200c are well above. Market samples of these medicines in 90%v/v ethanol were obtained from two reputable manufacturers: SBL, India, and Dr. Willmar Schwabe India (WSI) Private Limited.

We examined the following physico-chemical aspects:

a. The presence of the physical entities in nanoparticle form and their size by Transmission Electron Microscopy (TEM) by bright-field and dark-field imaging.
b. Their identification by matching the Selected Area Electron Diffraction (SAED) patterns against literature standards for the corresponding known crystals.
c. Estimation of the levels of starting metals by a 500-fold concentration of medicines, followed by chemical analysis using Inductively Coupled Plasma-Atomic Emission Spectroscopy (ICP-AES).

Materials and methods

Materials

The homeopathic medications used for the purpose of research were obtained commercially from authorized distributors of a leading homeopathic drug manufacturer in India (SBL) and an Indian subsidiary of a multi-national homeopathic company viz. Dr. Willmar Schwabe India Pvt. Ltd. Random batch number samples were purchased from the market and no special effort was made to get samples from the company. Since we purchased these medicines from the market, only in certain cases were we able to obtain them from a single manufacturing batch. Also no special efforts were made to obtain the drugs from a batch. The High-performance liquid chromatography (HPLC) grade ethanol used for the purpose of ICP-AES analyses was procured from Commercial Alcohols Inc., Canada. The TEM grids obtained from Pacific Grid-Tech (USA) were 200 mesh copper grids coated with carbon−formvar.

Methods

Nanoparticle characterization by TEM/SAED: The TEM analyses were performed on Tecnai G2 120 kV Cryo-TEM (FEI, Hillsboro, USA). All samples were viewed at 120 kV. The TEM analyses were performed for the medicines by placing a drop of the original solution (without pre-concentration) on the carbon−formvar coated copper TEM grids in a clean environment. The drop of the solution was then allowed to dry completely after which another drop was added. The usual drying time for each drop was approximately 30−60 min in air at room temperature. This procedure was repeated 5 times. After air-drying the sample for further 30−60 min, the grid was kept under an IR lamp for approximately 20 min to ensure complete drying of the sample and thereby preventing the possibility of solvent molecules from adhering to the particles on the grid. The SAED patterns of the particles were taken and the d-spacings were calculated using the camera length (calibrated daily using a standard gold colloid). The dark-field images were also taken by selecting three spots from two inner rings on the SAED pattern. The d-spacing values from SAED patterns and the crystallite sizes from the dark-field images were calculated using the Image-J software.

Elemental composition by ICP-AES: The determination of the starting elements in ultra-trace concentrations was performed on Ultima 2, (Jobin Yvon Horiba, Japan). The operating parameters for the ICP-AES instrument were as follows: plasma gas flow rate (Argon gas): 12 l/min; auxiliary gas flow rate: 0.2 l/min; sample uptake: 2.5 ml/min; integration time: 5.0 s, Spray Chamber: cyclonic chamber. The limit of detection of the instrument was 10 ppb. For the purpose of ICP-AES analyses, the samples were prepared by pre-concentrating the solutions (6c, 30c, and 200c potencies) 500-fold in a vacuum rotary evaporator, Roteva Model #8706R (Equitron, India) at 45°C and 100 rpm speed.

The homeopathic medicines that we purchased were in either 100 ml or 500 ml capacity bottles. Most of the SBL homeopathic medicine bottles were of 500 ml capacity with a few of 100 ml capacity, while those obtained from Willmar Schwabe India (WSI) Pvt. Ltd. were all 100 ml bottles. In the case of medicines obtained as 500 ml bottles, solutions from 4 bottles of the same medicine and potency were pooled together for concentration, whereas for medicines which were marketed as 100 ml bottles, solutions from 20 bottles of each medicine at the same potency were pooled. The concentration was carried out in a 50 ml clean round bottom flask on a rotary vacuum evaporator. The flask was filled with the solution (approximately 30−35 ml at a time) and the solvent was evaporated. Upon complete evaporation of the solvent, the flask was refilled with fresh homeopathic solution and the process was repeated till the entire volume of 2000 ml was evaporated. Only one bottle was opened at a time to maintain the integrity of the purchased medicines. To prevent contamination, under no circumstances was the solution in the bottle kept exposed. The residues of *Cuprum met*, *Stannum met*, and *Zincum met* were acidified to solubilize the particles of their respective starting metals by addition of concentrated nitric acid. Similarly, aqua regia (concentrated nitric acid and concentrated hydrochloric acid in the ratio 1:3) was added to residues of *Aurum met*, *Argentum met*, and *Platinum met*. A 1:1 ratio of water: acid was maintained for all the concentrated samples. The amount of acid and water was adjusted so that the final volume was 4 ml, thus, amounting to a concentration by a factor of 500. The samples were filtered

through Whatman 40 filter paper to remove the residual matter prior to analysis. The SBL samples were analyzed in triplicate and samples from WSI were analyzed in duplicate. As a negative control, 90%v/v ethanol samples were also prepared using HPLC grade ethanol and Milli-Q water. These ethanolic solutions were also concentrated in the manner similar to that employed for the medicines.

The emission lines selected for measuring the concentration of the metals are as follows: Gold: 242.795 nm, Copper: 324.754 nm, Tin: 283.999 nm, Zinc: 213.856 nm, Silver: 328.068 nm, Platinum: 265.945 nm. The instrument response was calibrated using standards prior to analyses of the samples.

Results and discussion

Determination of size and morphology by TEM

Zincum met, *Aurum met*, *Stannum met* and *Cuprum met* 30c and 200c were analyzed by TEM. The results are given as photomicrographs (Figure 1(a)−(p)), which clearly demonstrate the presence of nanoparticles and their aggregates. Due to extreme dilution often only a single nanoparticle or a large aggregate is seen. Hereafter, the term 'particles' collectively refers to the nanoparticles and their aggregates.

We noted a high polydispersity of the particles in the solutions with respect to their shapes and sizes for various medicines and potencies. A scrupulous examination of the entire manufacturing process of these medicines suggested that two key processes played a vital role in imparting the high polydispersity. They are:

1. The dilution steps in the solid phase (till 6× potency) involved trituration of the raw materials with lactose. Such a comminution process is expected to generate particles of varied shapes and sizes. The physical characteristics of these particles are dependent on the type of raw material and the shearing force applied.
2. During liquid dilutions, the succussion process at each potentization step played a vital role. The succussions given to the liquid mass are expected to produce particles of varied shapes and sizes due to three factors including shearing forces generated during the pounding of the liquid container against an elastic stop, the properties of the raw materials involved, and variations during pounding of the container, between individuals.

The permutations and combinations of the above-mentioned factors and the possible subtle differences in the manufacturing processes employed by various manufacturers can explain the findings regarding polydispersity between different medicines and manufacturers.

We also made another prominent observation regarding the presence of surface asperities on the particles which were clearly evident from the differences in contrast on surfaces of these particles along with a substantial difference in their size between different starting metals. Thus, larger aggregates were found in *Zincum met* (Figure 1(a)−(d)) and *Stannum met* (Figure 1(i)−(l)) as compared to those observed in *Aurum met* (Figure 1(e)−(h)) and *Cuprum met* (Figure 1(m)−(p)) at the same potencies.

The mechanism of cavitation or generation of vapor bubbles caused by ultra-sound irradiation (acoustic cavitation) in the entire liquid mass during manufacturing may explain the observations noted above. We suggest that the process of succussion is the cause of cavitation. As set out in a later section, the extant theories of cavitation[11−14] can, in principle, provide an explanation of our findings.

The aggregation behavior of the particles seems to be dependent on the physical property of the starting metal, specifically its melting point. We observed that the aggregates of zinc in *Zincum met* and tin in *Stannum met* were relatively larger as compared to the smaller aggregates of gold and copper found in *Aurum met* and *Cuprum met* respectively. The bulk melting points of tin and zinc are ∼505 K and ∼692 K respectively as compared to the higher melting points of gold and copper (∼1337 K and ∼1357 K respectively). A decrease in melting points of metallic and semiconductor particles with decreasing size has also been well characterized.[15] A combination of extremely high surface temperatures along with a decrease in the melting point of these particles could facilitate the formation of aggregates that we found.

It is probable that during the succussion process, the collisions of the particles induce surface temperatures well above the melting points of tin and zinc, thereby facilitating their aggregation. However, the melting points of gold and copper being much higher, the occurrence of melting and fusion of these particles would be relatively less frequent than for tin and zinc.

Overall, our data for bright-field TEM do not indicate a major difference in the size or nature of the particles in a particular medicine as we increase potency from 30c to 200c. Therefore, the individual crystallite sizes were determined by dark-field TEM (as shown for *Zincum met* for both manufacturers in Figure 2(a)−(d)). We observed that the aggregates of all the metals tested had maximum crystallites (∼40−50%) in the size range of 5−10 nm, and that 70−95% of all the crystallites were below 15 nm (Figure S1 − Supplementary information). Thus, in the case of dark-field TEM also, there was no major potency-dependent difference in size distribution of crystallites.

Confirmation of elemental composition of particles by SAED

The nanoparticles and aggregates identified in TEM were analyzed by SAED for confirmation of the elemental composition. We took multiple SAED patterns of the same particle at varying intensities so as to focus on the inner and outer rings for calculation of the d-spacings of the respective elements. The SAED patterns of the nanoparticles and their aggregates found in the metal-based homeopathic medicines are represented in Figure 3(a)−(p).

SAED analyses of all samples showed patterns consistent with the starting materials. In particular, *Aurum met* and *Cuprum met* from both suppliers (SBL and WSI) indexed to gold and copper respectively. Table 1 shows the values of the d-spacings calculated from the diameters of

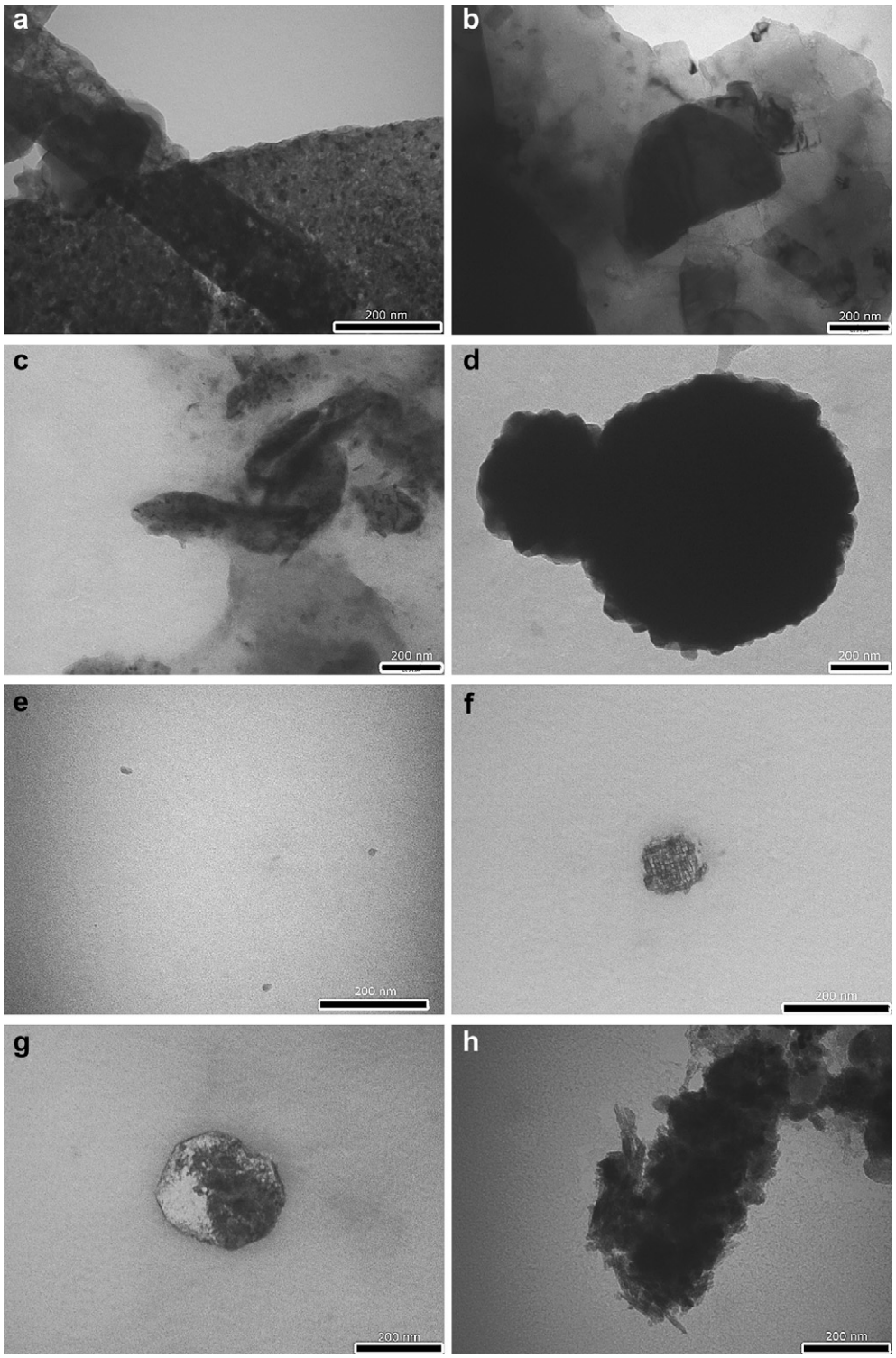

Figure 1 Bright-field TEM images of nanoparticles and aggregates. *Zincum met*: (**a**) 30c (SBL), (**b**) 200c (SBL), (**c**) 30c (WSI), (**d**) 200c (WSI). *Aurum met*: (**e**) 30c (SBL), (**f**) 200c (SBL), (**g**) 30c (WSI), (**h**) 200c (WSI). *Stannum met*: (**i**) 30c (SBL), (**j**) 200c (SBL), (**k**) 30c (WSI), (**l**) 200c (WSI). *Cuprum met*: (**m**) 30c (SBL), (**n**) 200c (SBL), (**o**) 30c (WSI), (**p**) 200c (WSI).

the ring patterns of particles observed in *Aurum met* samples. Similarly, in the case of *Stannum met* from SBL, the observed pattern indexed to α-Sn whereas that from WSI to β-Sn. In the case of *Zincum met* samples from both suppliers, we did not observe pure metallic zinc, but the SAED patterns indexed to zinc hydroxide which is an expected compound derived from zinc (d-spacing data for zinc, tin and copper have been given as Supplementary information – Tables S2–S5).

The confirmed presence of these crystalline species of starting materials or those derived from them (as evident from the SAED patterns) despite the ultra-high dilutions

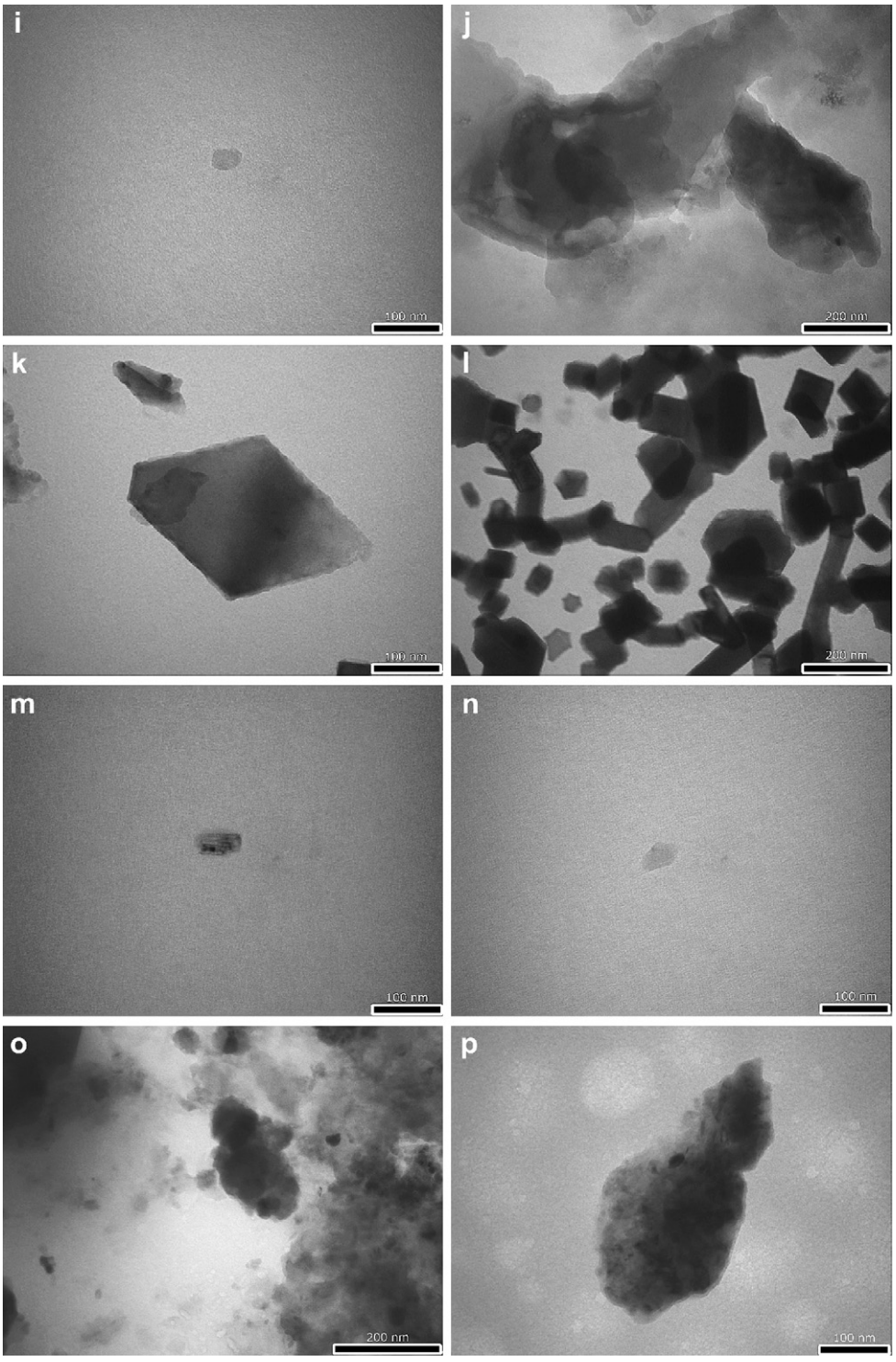

Figure 1 (*continued*).

such as 30c and 200c was astounding, proving that the starting materials were retained even with extremely high dilutions.

The d-spacing values for the particular elements conformed well to the Joint Committee on Powder Diffraction Standards (JCPDS) data in literature in the range of ±2%. However, for some d-spacings corresponding to a few planes in the crystal, the values differed by approximately ±4%. The differences in some of the d-spacing values for each metal can be explained on the basis of induction of minor plastic deformations in the crystals. The initial trituration process involving high shearing forces, together with the succussion process involving high-velocity collisions of nanoparticles resulting in the generation of shock waves caused by the imploding cavitations, may have induced minor plastic deformations in the metal crystals.

In a few of the SAED patterns for the metals analyzed, the particles also showed presence of diffused ring

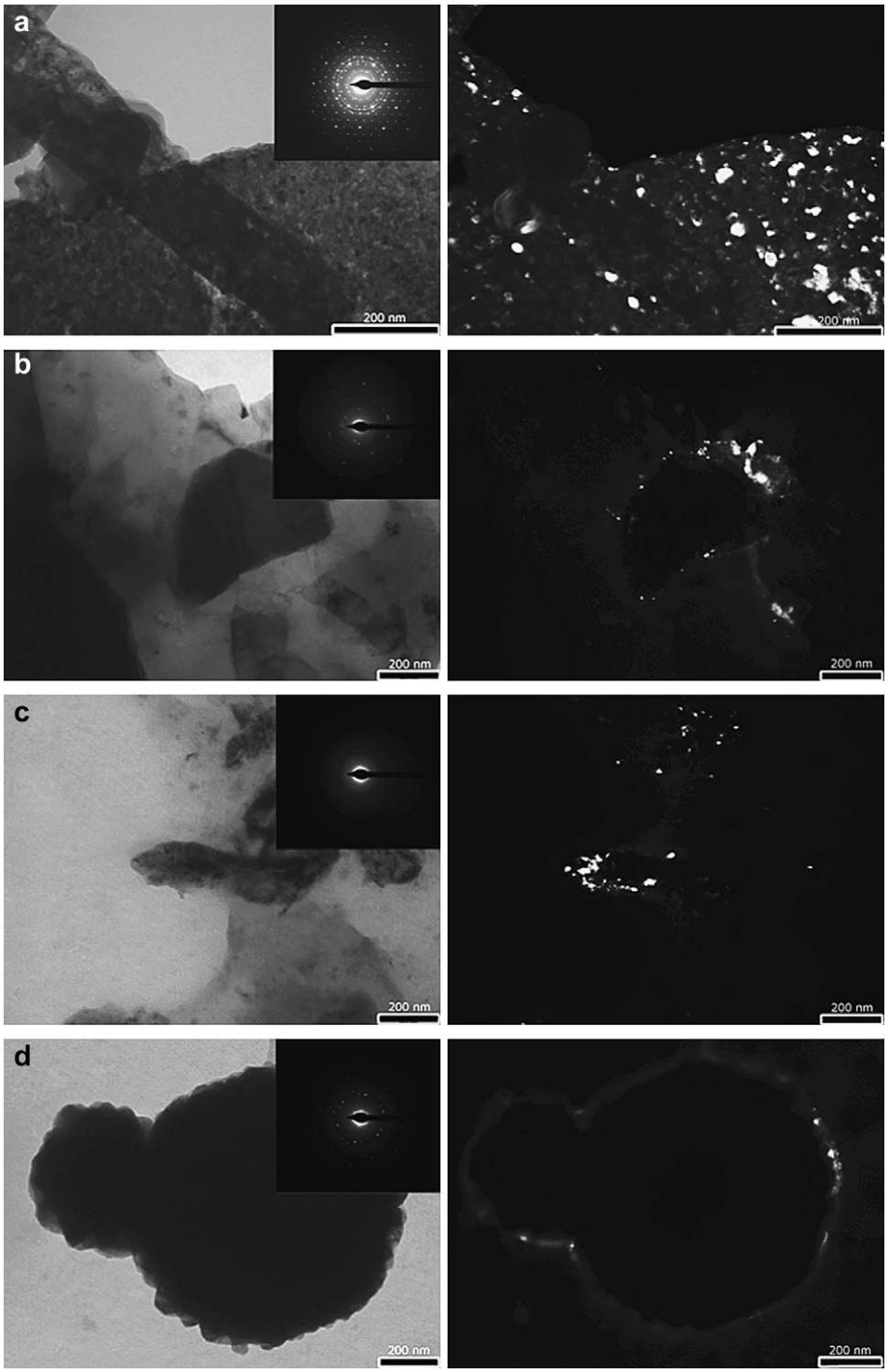

Figure 2 Bright-field and corresponding dark-field TEM images of nanoparticles and aggregates observed in *Zincum met*: (**a**) 30c (SBL), (**b**) 200c (SBL), (**c**) 30c (WSI), (**d**) 200c (WSI). Inset – SAED patterns of the corresponding nanoparticle/aggregate.

patterns similar to that of an amorphous material. The probable reason for presence of amorphous phases on the surface of the nanoparticles and aggregates is described later in this paper. On the whole, the SAED data indicated that the particles of the starting materials were present in the homeopathic medicines even in potencies such as 30c and 200c. In order to quantify the exact amounts of these starting metals in ultra-high potencies, we conducted the ICP-AES analyses of these medicines.

Estimation of concentration of the starting materials by ICP-AES

ICP-AES is an established technique for the estimation of metals and other elements. Our equipment had a minimum detectable limit of 10 ppb, thereby necessitating

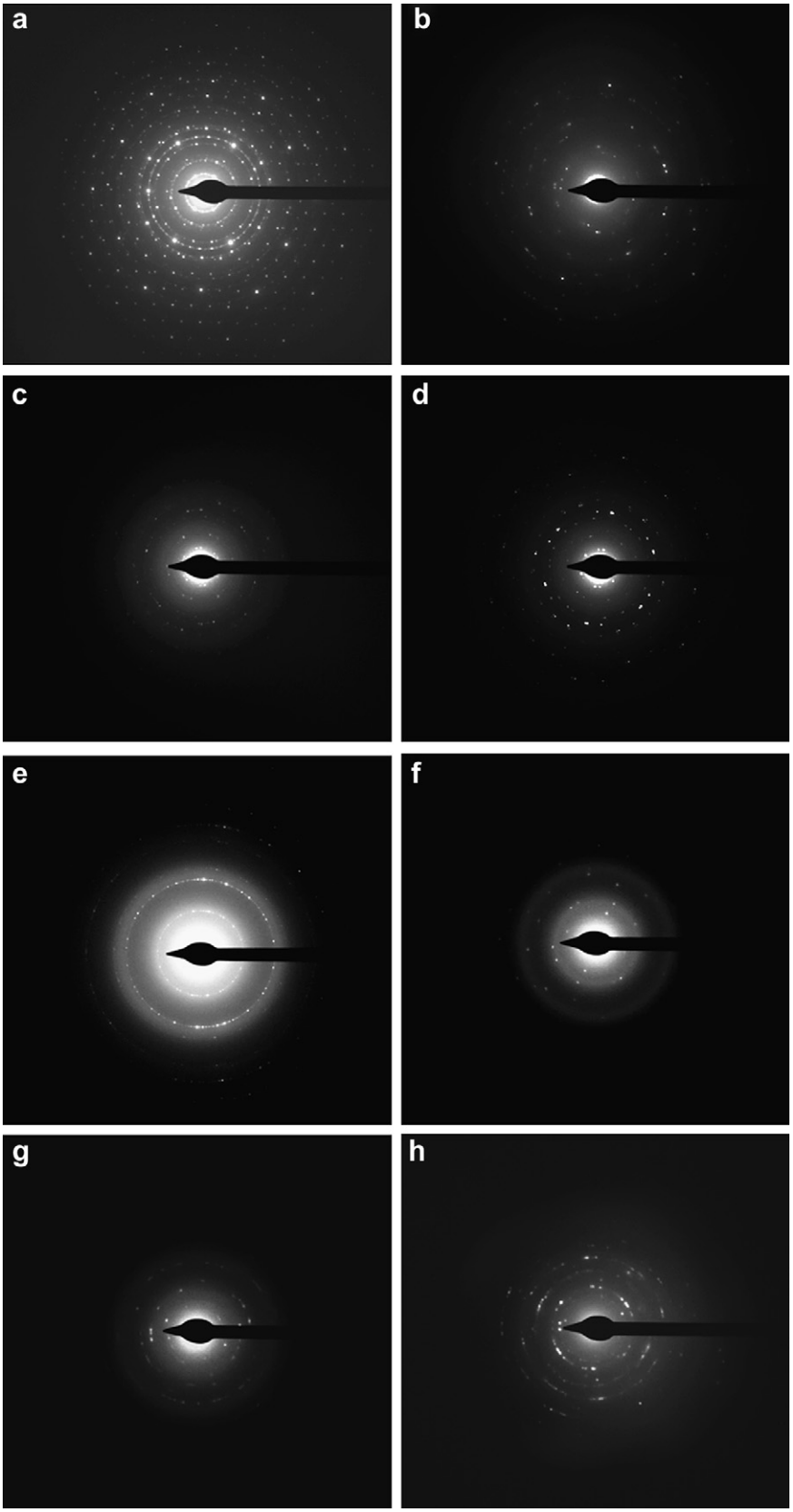

Figure 3 SAED patterns of corresponding nanoparticles and aggregates (shown in Figure 1(a)–(p)). *Zincum met*: (**a**) 30c (SBL), (**b**) 200c (SBL), (**c**) 30c (WSI), (**d**) 200c (WSI). *Aurum met*: (**e**) 30c (SBL), (**f**) 200c (SBL), (**g**) 30c (WSI), (**h**) 200c (WSI). *Stannum met*: (**i**) 30c (SBL), (**j**) 200c (SBL), (**k**) 30c (WSI), (**l**) 200c (WSI). *Cuprum met*: (**m**) 30c (SBL), (**n**) 200c (SBL), (**o**) 30c (WSI), (**p**) 200c (WSI).

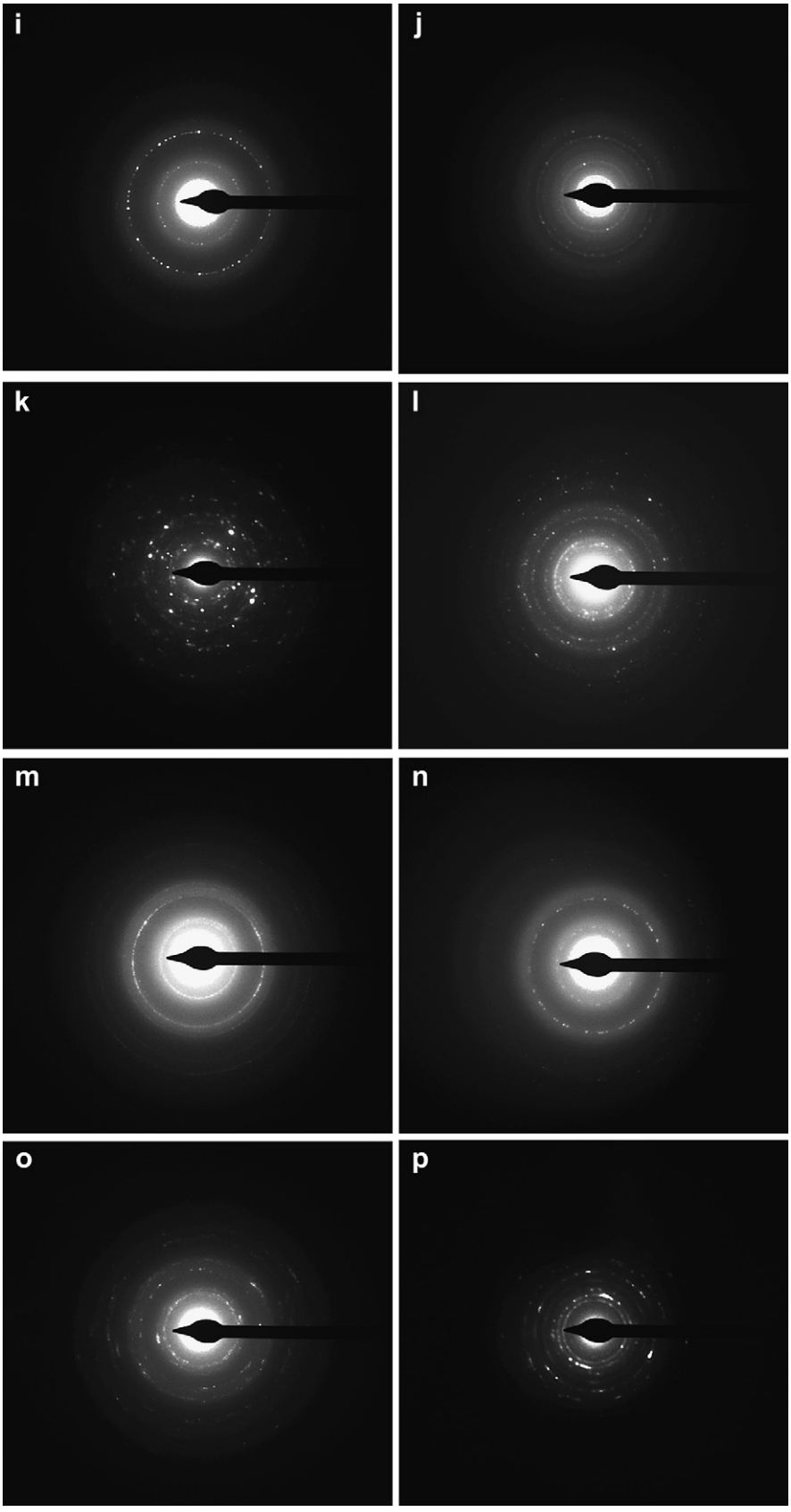

Figure 3 (*continued*).

Table 1 Electron diffraction pattern – comparison of d-spacing for *Aurum met* 30c and 200c potencies

hkl values	*Relative intensity*	*d-spacing Gold [Å]*	Aurum met *30C SBL – Figure 3(e)*	Aurum met *200C SBL – Figure 3(f)*	Aurum met *30C WSI – Figure 3(g)*	Aurum met *200C WSI – Figure 3(h)*
111	**100**	**2.3550**			2.3515	2.3312
200	**52**	**2.0390**	2.0300	2.0393	2.0213	2.0224
220	**32**	**1.4420**		1.4389	1.4454	1.4418
311	**36**	**1.2300**	1.2000	1.2598		1.2514
222	**12**	**1.1774**		1.1809	1.1732	1.1695
400	**6**	**1.0196**	1.0700	1.0072	1.0152	1.0211
331	**23**	**0.9358**				0.9530
420	**22**	**0.9120**		0.9120	0.9079	
422	**23**	**0.8325**			0.8286	
333	–	0.7850	0.7600	0.7843		
440	–	0.7210		0.7179	0.7196	
531	–	0.6890		0.6939		
442	–	0.6800				
620	–	0.6450	0.6600			
533	–	0.6220				
622	–	0.6150				
444	–	0.5890				

All d-spacing values are in Å units. d-spacing data in '**bold**' – from JCPDS#04-0784, remaining d-spacing data from Edington.[16]

concentration of the homeopathic solutions using a technique in which there is absolutely no possibility of adding inadvertently the metal to be detected.

The analyses of the metal-based medicines, performed after the concentration of the solutions gave startling results. The starting metals were detected for all potencies (6c, 30c, and 200c) at concentrations of the order of picogram/ml (pg/ml). The measured concentrations are presented in Table 2. The data presented in the table are back-calculated concentrations of the metals in the original homeopathic medicines. The analyses of the negative control of 90%v/v ethanol did not indicate the presence of either the noble metals or tin, and for metals such as copper and zinc, indicated far lower concentrations than those in the medicines.

We analyzed several samples of *Aurum met*, *Argentum met*, and *Platinum met* for the presence of their respective starting metals. In the case of *Aurum met* (SBL), some of the samples tested, including higher potencies such as 30c and 200c indicated presence of approximately 60–100 pg/ml of gold; the levels being much higher than the sensitivity of the instrument whereas in the ethanol–water negative controls there was no signal for the presence of gold. However, a few *Aurum met* (SBL) samples did not show presence of gold. Our results point towards a considerable batch-to-batch variation in the concentrations of the starting material. This is certainly not surprising, considering that the method of preparation involved manual processes along with an absence of any attempt to estimate the concentrations of the starting materials at the end of the manufacturing process of a particular batch. The *Aurum met* (WSI) samples did not show gold in detectable quantities.

Analogous results were obtained for the *Argentum met* (SBL) samples wherein silver was detected in one 30c and one 200c sample (30.6 pg/ml and 116 pg/ml respectively). The concentrations in the other samples were below the detection limit. Likewise, we discerned detectable concentration of platinum (~40–220 pg/ml) in the *Platinum met* (SBL) samples for all potencies.

The concentrations of non-noble metals such as copper, tin and zinc in their respective homeopathic medicines viz. *Cuprum met*, *Stannum met*, and *Zincum met* were higher (2–30 times that of noble metals) and easily detectable. In the *Cuprum met* samples (SBL), we detected ~500–2500 pg/ml of copper in the solutions. Similarly, 6c potency of WSI indicated high concentration of copper (~370 and ~900 pg/ml respectively in the two samples). However, the concentrations of copper in the higher potencies viz. 30c and 200c were very low (~10–40 pg/ml) in some and below detectable limits in the others. Likewise for *Stannum met* samples (SBL) we detected tin; albeit with very high variations from ~70 to 1000 pg/ml. In the WSI homeopathic solutions of *Stannum met* however, lower concentrations of tin were detected in the range of ~20–180 pg/ml. As compared to the other samples of non-noble metals noted above, the concentration of zinc in the *Zincum met* samples was much higher. In the *Zincum met* samples we detected presence of zinc with a very high variation in the concentrations between manufacturers from ~200 to 2700 pg/ml and ~1400 to 4000 pg/ml for SBL and WSI respectively.

It was reassuring that there was good reproducibility in terms of the estimated concentrations of the starting materials in the pair of samples of the same medicine, potency, and the manufacturing batch. We observed a variation up to 40% in the samples prepared from the same manufacturing batch as compared to a variation up to 1550% in samples from different batches. These results clearly highlighted the following:

1. Validation of the accuracy of our method involving preconcentration of the medicines prior to analyses as exemplified by the moderate variation in intra-batch samples (refer data sets for *Cuprum met*, *Stannum met*, and *Zincum met* marked in bold in Table 2).
2. High inter-batch variation in the concentration of the starting materials for a given manufacturer and potency, and between manufacturers.

Table 2 Estimated concentration of starting metals in various potencies by ICP-AES (pg/ml)

Homeopathic dilution	*SBL (pg/ml)*			*WSI (pg/ml)*	
	1	*2*	*3*	*1*	*2*
90%v/v Ethanol	**ND**	**ND**	**ND**	**ND**	**ND**
Aurum met 6c	81.4	76.4	ND	Samples not obtained	
Aurum met 30c	64.8*	ND	58.2	ND	ND
Aurum met 200c	ND	104.6	ND	ND	ND
90%v/v Ethanol	153.4	**245.0**	**149.0**	**245.0**	**149.0**
Cuprum met 6c	**1199.0**	**995.2**	1355.6*	893.4	370.8
Cuprum met 30c	**730.2**	**703.2**	1383.4*	38.6*	ND
Cuprum met 200c	**485.4**	**432.2**	2680.2*	**ND**	**ND**
90%v/v Ethanol	**ND**	**ND**	**ND**	**ND**	**ND**
Stannum met 6c	**569.4**	**409.2**	195.8*	**180.8**	**153.0**
Stannum met 30c	**901.6**	**889.6**	145.6	**93.8**	**76.4**
Stannum met 200c	**877.8**	**1055.8**	63.8*	20.8	73.0
90%v/v Ethanol	**208.2**	**210.2**	**199.0**	**208.2**	**210.2**
Zincum met 6c	**380.0**	**366.0**	1002.8	1432.6*	3989.6
Zincum met 30c	655.2	165.4	1224.0	3068.6*	1377.6
Zincum met 200c	357.8	191.2*	2743.6	2230.2*	2322.8
90%v/v Ethanol	**ND**	**ND**	**ND**		
Argentum met 6c	ND	ND	30.6	Samples not obtained	
Argentum met 30c	ND	116.0	ND		
Argentum met 200c	ND	ND	ND		
90%v/v Ethanol	ND				
Platinum met 6c	220.6*	Samples not obtained		Samples not obtained	
Platinum met 30c	41.0*				
Platinum met 200c	213.6				

'**Bold**' against a pair of samples in a row for given manufacturer and potency indicates their preparation from same manufacturing batch. The Limit of Detection (LOD) of the instrument was 10 ng/ml corresponding to 20 pg/ml in the original solutions. All concentrations below this value have been reported as 'Not Detected' or 'ND'.
* Data indicate that the bottles used to make up the required quantity (2000 ml) were from the same manufacturing batch.

Thus, for each metal-based medicine of a particular potency, the estimated values appeared to be within a band of 2 orders of magnitude. These variations could be attributed to the processes employed for manufacturing. A visit to a reputed manufacturer revealed that the initial lactose triturations were performed on an automated machine using a mortar and pestle. Apart from the control of particle sizes of the metal powders at 1× potency (wherein 80% of the particles of the starting material should be below 10 μm and none above 50 μm),[17] there are no further checks for the distribution of the metals in the triturated 6× mixture, which is the starting material for proceeding to the liquid based succussion steps. This is believed to be the cause of these large variations.

The liquid dilutions and the potentization steps (including succussion) were done manually during manufacturing, wherein the entire mass of the liquid in the glass container was pounded against a rubber stop 10 times, with inevitable variation in the force of impact and the extent of cavitation generated during these human powered succussions. Apart from the initial trituration with lactose, succussion *per se* could also be an important method of generation of nanoparticles of the starting materials, due to intense shearing of these nanoparticles against the walls of the glass containers, by the fluid shear and possibly by particle collision due to the implosion of the cavitations created by the ultra-sound waves generated. Therefore, a difference in the shearing force imparted during succussion could result in a large difference in the formation of the nanoparticle fraction of the starting materials, thereby reflecting as inter-batch variation.

Once the succussion process was completed, the entire mass of liquid was allowed to settle, prior to transfer of 1% of this dilution to 99 parts fresh 90%v/v ethanol. However, the settling time for the dilutions was not fixed. Also, the removal of one part of the previous dilution for the purpose of transferring into a fresh solvent was carried out randomly from the container and was a manual process. All the above-mentioned factors combined are expected to impart a lot of disparity in the concentrations of the starting materials in the final medicines which we observed in our studies.

During our analyses we also noted the plateauing effect of the concentrations of the starting metals per se in a particular concentration range in potencies 6c, 30c and 200c, in spite of 30c and 200c potencies being 10^{48} and 10^{388} respectively more dilute than 6c. It is interesting to note that the plateau for non-noble metals showed a higher metal content than for noble metals. Our ICP-AES results suggested that the asymptote effect commences around 6c potency (Figure 4).

Our findings appear to be an extension of the trends noted at lower potencies by Röder *et al.*,[18] who analyzed the concentrations of a few metals in decimal dilutions from 6× to 8× (corresponding to centesimal potencies of 3c to 4c). Part 'A' in Figure 4 explicitly depicts decrease in the concentrations of starting materials with dilutions. Only in the case of Au^{3+} in $AuCl_3$ solutions, the

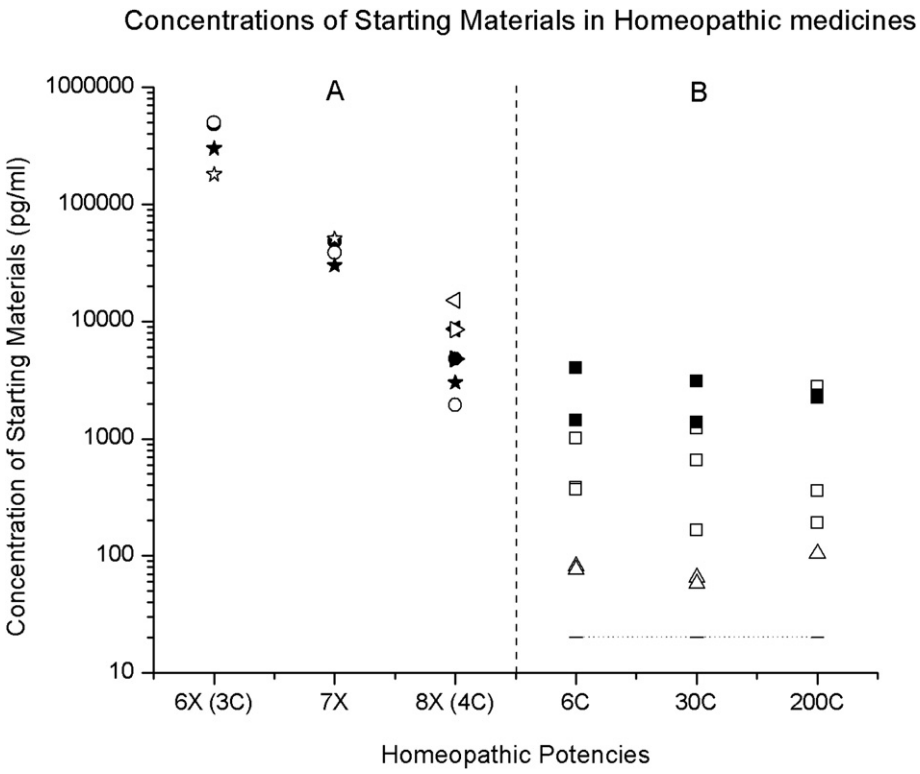

Figure 4 Estimated concentrations of starting elements in homeopathic potencies. **Part 'A'** – estimated by Röder *et al.*[18] – solid symbols: expected concentrations, open: estimated concentrations, circles: Au^{3+}, star: Fe^{3+}, left triangle: Hg^{2+}, right triangle: Zn^{2+}. **Part 'B'** – estimated by ICP-AES in our work – squares: zinc concentrations, open: *Zincum met* (SBL), solid: *Zincum met* (WSI), open triangles: gold concentrations in *Aurum met* (SBL) samples. The dotted line at 20 pg/ml indicates the LOD of the instrument.

actual concentrations determined were lesser than the expected concentrations (circles, solid: expected; open: estimated concentrations). On the contrary, the concentrations of Fe^{3+} though slightly lower than expected at the 6× potency, did not decrease as expected, and were in fact slightly higher at 7× and 8× potencies (stars, solid: expected; open: determined concentrations). Likewise, the concentrations of Hg^{2+} and Zn^{2+} were almost 200% higher than expected at 8× potency. A scrupulous, concurrent analysis of these results suggested the commencement of an asymptote formation in the vicinity of the 8× (i.e. 4c) potency.

When the data from Part 'A' of the graph are compared with our data (Part 'B'), there appears to be a plateauing effect, reached at 6c potency.

While a plateau is reached for each metal, the concentration range varied from one metal to another and between manufacturers. The plateau of *Zincum met* (WSI) (solid squares) was appreciably higher (between 1300 and 4000 pg/ml) than that for *Zincum met* (SBL) (open squares), albeit with the inherent variation mentioned earlier. Similar trends were also observed for all the other metals that were analyzed.

Possible key mechanisms at large dilutions

Acoustic cavitation, a well studied phenomenon[11–14] may explain our TEM findings regarding surface asperities and particle aggregation. Researchers have observed that the vapor bubbles generated due to the high-energy sound waves had temperatures exceeding a few thousand degrees (~5000 K) along with intense pressures (~1000 atm). The bubbles so formed had very short lives before imploding, creating intense shock waves which propel particles in the solution at extremely high velocities resulting in collisions which induced the following morphological changes on the particle surfaces:

1. When the particles collided head-on, localized melting occurred on their surfaces at the point of contact, with the temperatures being ~3000 K. With the surrounding liquid at ambient temperature, the melted surfaces instantly cooled at extremely high rates (>10^{10} K/s), thereby solidifying the melted area instantaneously and fusing the particles at the point of contact to form aggregates.
2. The extremely high rate of cooling, while not allowing for re-crystallization at the point of contact, led to an amorphous phase on the particle surface as evident from the diffused rings obtained in the electron diffraction (ED) patterns.
3. Collision of particles at a glancing angle led to fragmentation of the particle surface which may have given rise to surface asperities.

The above theories support our observations regarding the presence of the surface asperities we see in TEM, since the forceful pounding of the glass containers during the succussion process may have been instrumental in generating the ultra-sound waves, resulting in their formation.

Another question that arises from our observations is how in spite of such huge dilutions the particles of the starting materials are retained even at 200c potency? The answer to this question could lie in the manufacturing process itself. We perceive that during the succussion process, the pounding of solutions against a rubber stop generates numerous nanobubbles[19] as a result of entrapment of air and cavitation due to generation of ultra-sound waves. The particles of the starting material instantaneously get adsorbed on the surface of these bubbles and cavitations. This phenomenon could be similar to the mechanism of formation of Pickering emulsions,[20–22] wherein the emulsified phase viz. air bubbles or liquid droplets are stabilized by a layer of particles.

This nanoparticle–nanobubble complex rises to the surface and can be within a monolayer once the total metal concentrations are well below 1 ppm (Table S6 – Supplementary information). It is this 1% of the top layer of the solution which is collected and added to the next vessel, into 99 parts of fresh solvent and the succussion process is repeated. This transfer of the top 1% layer in each step will ensure that once we reach below a certain concentration i.e. well within a monolayer, the entire starting material continues to go from one dilution to the next, resulting in an asymptote beyond 6c.

Conclusion

Using state-of-the-art techniques (TEM, SAED, and ICP-AES) we have demonstrated the presence of nanoparticles of the starting materials and their aggregates even at extremely high dilutions. The confirmed presence of nanoparticles challenges current thinking about the role of dilution in homeopathic medicines. We have found that the concentrations reach a plateau at the 6c potency and beyond. Further, we have shown that despite large differences in the degree of dilution from 6c to 200c (10^{12} to 10^{400}), there were no major differences in the nature of the particles (shape and size) of the starting material and their absolute concentrations (in pg/ml).

How this translates into change in biological activity with increasing potency needs further study. Concrete evidence of the presence of particles as found by us could help take the research in homeopathy a step forward in understanding these potentised medicines and also help to positively change the perception of the scientific community towards this mode of treatment.

Conflict of interest

There are neither any financial nor any personal conflicts of interest with respect to the work carried out for this article.

Acknowledgements

We thank the Department of Earth Sciences and the Cryo-TEM central facility at IIT Bombay for ICP-AES and TEM analyses respectively. We also gratefully acknowledge funding by Shridhar Shukla, S G Kane and Industrial Research and Consultancy Center (IRCC), IIT Bombay. We also thank P N Varma for valuable insights.

Supplementary data

Supplementary data associated with this article can be found in the online version at doi:10.1016/j.homp.2010.05.006.

References

1 Khuda-Bukhsh AR. Laboratory research in homeopathy: Pro. *Integr Cancer Ther* 2006; **5**: 320–332.
2 Khuda-Bukhsh AR. Towards understanding molecular mechanisms of action of homeopathic drugs: an overview. *Mol Cell Biochem* 2003; **253**: 339–345.
3 Davenas E, Beauvais F, Amara J, *et al*. Human basophil degranulation triggered by very dilute antiserum against IgE. *Nature* 1988; **333**: 816–818.
4 Chaplin MF. The memory of water: an overview. *Homeopathy* 2007; **96**: 143–150.
5 Teixeira J. Can water possibly have a memory? A skeptical view. *Homeopathy* 2007; **96**: 158–162.
6 Anagnostatos GS. Small water clusters (clathrates) in the homoeopathic preparation process. In: Endler PC, Schulte J (eds). Ultra High Dilution – Physiology and Physics. Dordrecht, the Netherlands: Kluwer Academic Publishers, 1994, p. 121–128.
7 Rao ML, Roy R, Bell IR, Hoover R. The defining role of structure (including epitaxy) in the plausibility of homeopathy. *Homeopathy* 2007; **96**: 175–182.
8 Walach H, Jonas WB, Ives J, van Wijk R, Weingärtner O. Research on homeopathy: state of the art. *J Altern Complement Med* 2005; **11**: 813–829.
9 Davydov AS. Energy and electron transport in biological systems. In: Ho MW, Popp FA, Warnke U (eds). Bioelectrodynamics and Biocommunication. Singapore: World Scientific Publishing Co. Pte. Ltd., 1994. Chap 17, pp 411–430.
10 Anick DJ, Ives JA. The silica hypothesis for homeopathy: physical chemistry. *Homeopathy* 2007; **96**: 189–195.
11 Doktycz SJ, Suslick KS. Interparticle collisions driven by ultrasound. *Science* 1990; **247**: 1067–1069.
12 Suslick KS, Doktycz SJ. The sonochemistry of Zn powder. *J Am Chem Soc* 1989; **111**: 2342–2344.
13 Suslick KS, Price GJ. Applications of ultrasound to materials chemistry. *Annu Rev Mater Sci* 1999; **29**: 295–326.
14 Suslick KS. The chemical effects of ultrasound. *Sci Am* 1989 (Feb);80–86.
15 Goldstein AN, Echer CM, Alivisatos AP. Melting in semiconductor nanocrystals. *Science* 1992; **256**: 1425–1427.
16 Edington JW. Philips technical library – monographs in practical electron microscopy in materials science 2 – electron diffraction in the electron microscope. Eindhoven: N.V. Philips', 1975, p 110.
17 Varma PN, Vaid I. Encyclopedia of homoeopathic pharmacopoeia & drug index. New Delhi: B. Jain Publishers, 2007, pp 2722–2745.
18 Röder E, Pütz W, Frisse R. Bestimmung von Au, Fe, Zn und Hg in homöopathischen Dilutionen durch zerstörungsfreie Neutronenaktivierungsanalyse. *Fresenius Z Anal Chem* 1981; **307**: 120–126.
19 Roy R, Tiller WA, Bell I, Hoover MR. The structure of liquid water: novel insights from materials research; potential relevance to homeopathy. *Mater Res Innov* 2005; **9**: 577–608.
20 Pickering SU. Emulsions. *J Chem Soc* 1907; **91**: 2001–2021.
21 Binks BP. Particles as surfactants – similarities and differences. *Curr Opin Colloid Interface Sci* 2002; **7**: 21–41.
22 Binks BP, Lumsdon SO. Influence of particle wettability on the type and stability of surfactant-free emulsions. *Langmuir* 2000; **16**: 8622–8631.